Cosmological probes of Gravity

Lecture 4: Testing the perturbative regimen of gravity with Large Scale Structure

Susana J. Landau[1,2]

[1]Departamento de Física - Facultad de Ciencias Exactas y Naturales - UBA
[2]Instituto de Física de Buenos Aires - CONICET - Universidad de Buenos Aires

1st Arica School on Cosmology and Gravitation
13-16 October 2026
Universidad de Tarapacá

Outline

1. Introduction to Large Scale Structure
2. Galaxy Clustering
3. Weak Lensing
4. Constraints on MG from WL, galaxy surveys and CMB
5. Relevant papers for this lecture
6. Appendix

The perturbative sector

- Let us now consider the FRW space-time with perturbations:

$$ds^2 = -(1+2\Psi_N)dt^2 + a^2(t)(1-2\Phi_N)\delta_{ij}dx^i dx^j \tag{1}$$

- In GR and in the absence of anisotropic stress, the two scalar potentials are equal: $\Phi_N = \Psi_N$. However, in modified gravity theories, this equality may not hold, leading to a gravitational slip between the two potentials : $\eta = \frac{\Phi_N}{\Psi_N}$.
- The newtonian potentials Φ_N and Ψ_N obey the modified Poisson equations:

$$\begin{aligned} k^2\Psi_N &= -4\pi G a^2(1+\mu(a,k))\rho\delta \\ k^2(\Phi_N+\Psi_N) &= -8\pi G a^2(1+\Sigma(a,k))\rho\delta \end{aligned} \tag{2}$$

- The functions $\mu(a,k)$ and $\Sigma(a,k)$ parametrize deviations from GR at the perturbative level.

Matter perturbation equation in MG

- The evolution of matter density perturbations in the subhorizon limit:

$$\ddot{\delta}_m + 2H\dot{\delta}_m + k^2\Psi_N = 0 \tag{3}$$

$$\ddot{\delta}_m + 2H\dot{\delta}_m - 4\pi \underbrace{G(1+\mu(a,k))}_{G_{\rm eff}} \rho_m \delta_m = 0 \tag{4}$$

- In this lecture we will analyze the observables are related to the solution of this equation:
  - The Power Spectrum $P(k)$
  - The Two-point correlation function $\xi(r)$
  - The quantity $f\sigma_8 = \frac{\partial \delta_m}{\partial \ln a}\sigma_8(z)$
  - The shear correlation functions ξ_+ and ξ_- which can be related to δ_m but also the Weyl potential $\Phi_N + \Psi_N$.
  - These quantities are not observed directly, but derived from observations of galaxies, cosmic shear

The coupled Boltzmann equations in ΛCDM

- For each Fourier mode, the perturbations of all species are coupled ($' \equiv d/d\eta$, with Ψ_N, Φ_N as in the metric above). For the photons:

$$\Theta' + ik\mu\Theta = \Phi_N' - ik\mu\Psi_N - \tau'\left[\Theta_0 - \Theta + \mu u_b - \frac{1}{2}\mathcal{P}_2(\mu)\Pi\right] \tag{5}$$

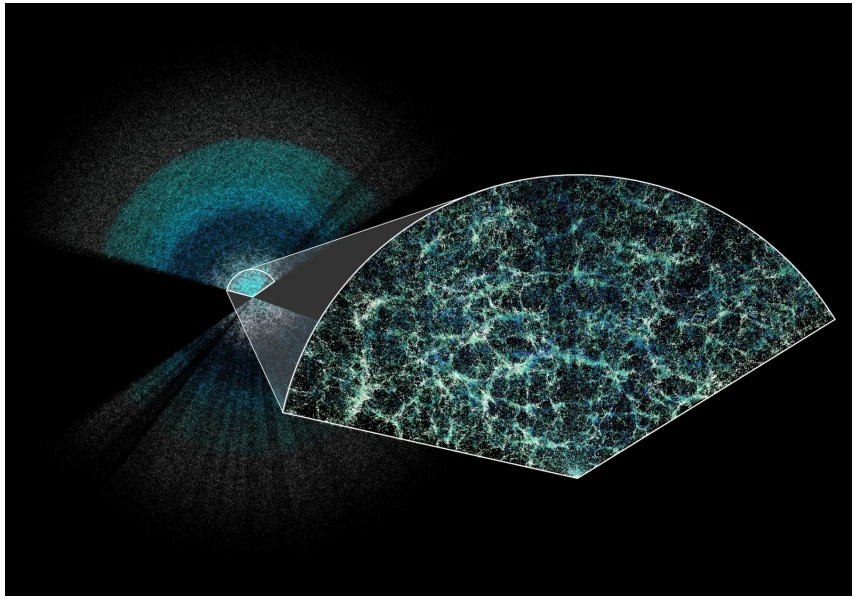
  with $\Pi = \Theta_2 + \Theta_{P,2} + \Theta_{P,0}$.

- Dark matter (density δ_c, velocity u_c), baryons and massive neutrinos:

$$\begin{aligned}
\delta_c' + iku_c &= 3\Phi_N' \\
u_c' + \frac{a'}{a}u_c &= -ik\Psi_N \\
\delta_b' + iku_b &= 3\Phi_N' \\
u_b' + \frac{a'}{a}u_b &= -ik\Psi_N + \frac{\tau'}{R}\left[u_b + 3i\Theta_1\right] \\
\mathcal{N}' + ik\mu\frac{p}{E_\nu(p)}\mathcal{N} - Hp\frac{\partial}{\partial p}\mathcal{N} &= \Phi_N' - ik\mu\frac{E_\nu(p)}{p}\Psi_N
\end{aligned} \tag{6}$$

- Dark matter couples to the other species only through gravity. In the case of modified gravity, the above equations should be modified accordingly in the framework of the specific MG model.

Large Scale Structure



- The large-scale structure (LSS) of the Universe is the characterization of the distribution of matter on scales much larger than individual galaxies.
- The LSS is a powerful probe of cosmology and gravity because it is sensitive to both the expansion history of the Universe and the growth of structure over time.
- Galaxy surveys map the distribution of galaxies over large volumes of the Universe: SDSS, BOSS, DES, KIDS, SUBARU, EUCLID, DESI, LSST.

Large Scale Structure

- We can distinguish between two main types of galaxy surveys:
  - Spectroscopic surveys: measure the redshifts of galaxies using spectroscopy. These surveys provide precise measurements of galaxy positions and redshifts, which makes them ideal for studying the clustering of galaxies. Examples: BOSS,DESI
  - Photometric surveys: measure the brightness of galaxies in multiple wavelength bands using imaging. These surveys provide less precise measurements of galaxy positions and redshifts, but can cover larger areas of the sky and reach fainter galaxies. Therefore, there are mainly used to measure cosmic shear. As a disadvantage, the measured redshift is less precise. Examples: DES,KIDS, LSST
- Photometric surveys can also be used for angular clustering of galaxies (2D), but the most precise measurements of BAO and RSD require spectroscopic redshifts. However, some modern surveys (such as DESI) include both spectroscopic and photometric components.
- Modern surveys such as DES, KiDS, Euclid, LSST are designed to measure both observables: (galaxy clustering and cosmic shear), but with different instrumental requirements and observational strategies.

Outline

1 Introduction to Large Scale Structure

2 Galaxy Clustering

3 Weak Lensing

4 Constraints on MG from WL, galaxy surveys and CMB

5 Relevant papers for this lecture

6 Appendix

Summary statistics

- Since $\langle X \rangle = 0$ for an overdensity field, the lowest-order non-trivial statistic is the two-point correlation function. In Fourier space:

$$\langle X(\mathbf{k_1}) Y(\mathbf{k_2}) \rangle = (2\pi)^3 \delta^3(\mathbf{k_1} + \mathbf{k_2}) P_{XY}(k_1) \tag{7}$$

it is related to the power spectrum, while in real space

$$\langle X(\mathbf{r_1}) Y(\mathbf{r_2}) \rangle = \xi_{XY}(|\mathbf{r_1} - \mathbf{r_2}|) = \int \frac{d^3k}{(2\pi)^3} P_{XY}(k)\, e^{i\mathbf{k}\cdot(\mathbf{r_1}-\mathbf{r_2})} \tag{8}$$

- The next statistic is the three-point correlation function, which measures the clustering of triplets of points. In Fourier space, it is related to the bispectrum:

$$\langle X(\mathbf{k_1}) Y(\mathbf{k_2}) Z(\mathbf{k_3}) \rangle = (2\pi)^3 \delta^3(\mathbf{k_1} + \mathbf{k_2} + \mathbf{k_3}) B_{XYZ}(\mathbf{k}_1, \mathbf{k}_2, \mathbf{k}_3) \tag{9}$$

while in real space

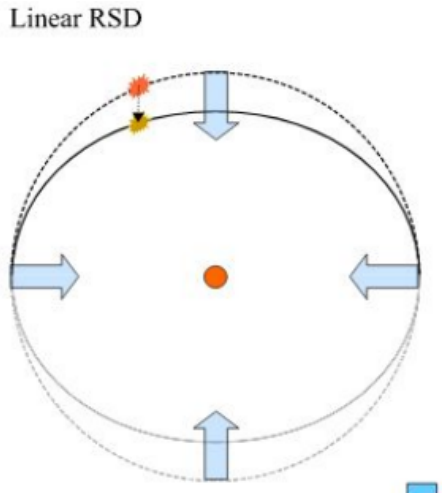
$$\begin{aligned} \langle X(\mathbf{r_1}) Y(\mathbf{r_2}) Z(\mathbf{r_3}) \rangle &= \zeta_{XYZ}(\mathbf{r}_1, \mathbf{r}_2, \mathbf{r}_3) \\ &= \int \frac{d^3k_1}{(2\pi)^3} \frac{d^3k_2}{(2\pi)^3} B_{XYZ}(\mathbf{k}_1, \mathbf{k}_2, -\mathbf{k}_1 - \mathbf{k}_2)\, e^{i(\mathbf{k_1}\cdot\mathbf{r_{13}} + \mathbf{k_2}\cdot\mathbf{r_{23}})} \end{aligned} \tag{10}$$

with $\mathbf{r}_{ij} \equiv \mathbf{r}_i - \mathbf{r}_j$.

Galaxy Clustering

- Galaxy Clustering surveys (BOSS, DESI) provide:
  - The angular positions of millions of galaxies (RA,DEC).
  - The redshifts of these galaxies.
- Some problems that can be addressed with these measurements are:
  - Bias: The galaxy clustering is different from the matter clustering.
  - The galaxy redshift contains both information about the cosmological redshift and the peculiar velocity of galaxies: Redshift Space Distortions
- In galaxy redshift surveys, each galaxy is located by its angular coordinates and redshift. However, the correlation function, $\xi(r_\perp, r_{||})$, is measured in comoving distances. Therefore a fiducial cosmological model is required for conversion into comoving space.
- Mock galaxy catalogs, which are essential for calculating covariance matrices are computed assuming ΛCDM + GR.

Redshift Space Distortions



- Due to the Doppler effect, the radial position of galaxies inferred from their redshifts is different from their true radial position.

$$z_{\rm obs} = z + \frac{v_{LoS}}{a} \tag{11}$$

where v_{LoS} is the line-of-sight component of the peculiar velocity of the galaxy. The shift in redshift lead to a shift in the comoving coordinates.

- This shift of redshift leads to that of the comoving coordinates:

$$\mathbf{s} = \mathbf{x} + \frac{v_{LoS}}{aH(a)}\hat{\mathbf{e}}_{\rm LoS} \tag{12}$$

where $\hat{\mathbf{e}_{\rm LoS}}$ is the unit vector along the line of sight.

Galaxy Overdensity in Redshift Space

- Let us define the galaxy overdensity field in redshift space as:

$$\delta_g(\mathbf{s}) = \frac{n_g(\mathbf{s}) - \bar{n}_g}{\bar{n}_g} \tag{13}$$

where $n_g(\mathbf{s})$ is the number density of galaxies at the redshift-space position $\mathbf{s}$ and $\bar{n}_g$ is the mean number density of galaxies.

- With these measurements the following statistical quantities can be obtained:
  - The galaxy two-point correlation function in redshift space :

$$\boxed{\xi_{gg}(s, \mu_s) = \langle \delta_g(\mathbf{s}')\delta_g(\mathbf{s}' + \mathbf{s}) \rangle} \tag{14}$$

where $s = |\mathbf{s}|$ is the galaxy separation and μ_s the cosine of its angle with the line of sight.

  - The galaxy power spectrum in redshift space (μ_k: cosine between $\mathbf{k}$ and the line of sight):

$$\boxed{\langle \delta_g(\mathbf{k})\delta_g(\mathbf{k}') \rangle = (2\pi)^3 \delta_D(\mathbf{k} + \mathbf{k}') P_{gg}(k, \mu_k)} \tag{15}$$

Matter clustering in real space

- The matter overdensity field in real space is defined as:

$$\delta_m(\mathbf{x}) = \frac{\rho_m(\mathbf{x}) - \bar{\rho}_m}{\bar{\rho}_m} \tag{16}$$

  where $\rho_m(\mathbf{x})$ is the matter density at position $\mathbf{x}$ and $\bar{\rho}_m$ is the mean matter density.

- The two-point correlation function in real space is defined as:

$$\xi_{mm}(r) = \langle \delta_m(\mathbf{x}) \delta_m(\mathbf{x}+\mathbf{r}) \rangle \tag{17}$$

  where $r = |\mathbf{r}|$ is the separation between two points in real space.

- Let us now define the Fourier transform of the matter overdensity field as:

$$\delta_m(\mathbf{k}) = \int d^3x \, \delta_m(\mathbf{x}) e^{-i\mathbf{k}\cdot\mathbf{x}} \tag{18}$$

- The two-point correlation function in Fourier space is defined as:

$$\langle \delta_m(\mathbf{k}) \delta_m(\mathbf{k}') \rangle = (2\pi)^3 \delta_D(\mathbf{k}+\mathbf{k}') P_{mm}(k) \tag{19}$$

Matter clustering in real space

- The two-point correlation function in real space is the Fourier transform of the power spectrum:

$$\xi_{mm}(r) = \int \frac{d^3k}{(2\pi)^3} P_{mm}(k) e^{i\mathbf{k}\cdot\mathbf{r}} = \frac{1}{2\pi^2} \int dk\, k^2 P_{mm}(k)\, j_0(kr) \qquad (20)$$

Redshift Space Distortions

- The anisotropic clustering $\xi(s, \mu_s)$ can be decomposed into multipoles using Legendre polynomials:

$$\begin{aligned} \xi_{gg}(s, \mu_s) &= \sum_{\ell} \xi_{\ell}(s) \mathcal{P}_{\ell}(\mu_s) \\ &\simeq \xi_0(s)\mathcal{P}_0(\mu_s) + \xi_2(s)\mathcal{P}_2(\mu_s) + \xi_4(s)\mathcal{P}_4(\mu_s) \end{aligned} \tag{21}$$

where $\xi_2(s)$ and $\xi_4(s)$ contain information about the growth rate defined as

$$f(z) = \frac{\partial \ln \delta_m}{\partial \ln a} \tag{22}$$

- $\xi_{gg}(\mathbf{s})$ and $P_{gg}(\mathbf{k})$ are a Fourier pair also in redshift space,

$$\xi_{gg}(\mathbf{s}) = \int \frac{d^3k}{(2\pi)^3} P_{gg}(\mathbf{k})\, e^{i\mathbf{k}\cdot\mathbf{s}} \tag{23}$$

Redshift Space Distortions

- The redshift-space power spectrum $P_{gg}(k, \mu_k)$ can be expressed as:

$$\boxed{P_{gg}(k, \mu_k) = b^2 \left(1 + \frac{f}{b}\mu_k^2\right)^2 P_{mm}(k) = (b + f\mu_k^2)^2 P_{mm}(k)} \tag{24}$$

where b is the linear bias, f is the growth rate, and μ_k is the cosine of the angle between the wave vector k and the line of sight.

- Expanding in Legendre polynomials, in linear theory only $\ell = 0, 2, 4$ survive:

$$P_{gg}(k, \mu_k) = \sum_{\ell=0,2,4} P_\ell(k)\, \mathcal{P}_\ell(\mu_k) \tag{25}$$

where

$$P_\ell(k) = \frac{2\ell + 1}{2} \int_{-1}^{1} d\mu_k\, P_{gg}(k, \mu_k)\, \mathcal{P}_\ell(\mu_k) \tag{26}$$

and

$$\xi_\ell(s) = i^\ell \int \frac{dk\, k^2}{2\pi^2} P_\ell(k)\, j_\ell(ks) \tag{27}$$

with j_ℓ the spherical Bessel functions.

- Writing $P_{mm}(k,z) = \sigma_8^2(z)\,\hat{P}(k)$, with $\hat{P}(k)$ the shape of the spectrum (normalized to $\sigma_8 = 1$):

$$
\begin{aligned}
P_0(k) &= \left[(b\sigma_8)^2 + \frac{2}{3}(b\sigma_8)(f\sigma_8) + \frac{1}{5}(f\sigma_8)^2\right]\hat{P}(k) \\
P_2(k) &= \left[\frac{4}{3}(b\sigma_8)(f\sigma_8) + \frac{4}{7}(f\sigma_8)^2\right]\hat{P}(k) \\
P_4(k) &= \frac{8}{35}(f\sigma_8)^2\,\hat{P}(k)
\end{aligned}
$$

- The multipoles depend only on the combinations $b\sigma_8$ and $f\sigma_8$: RSD measure $f\sigma_8(z)$, a direct probe of the growth of structure and therefore of gravity.

$f\sigma_8$ FROM RSD

- The quantity σ_8 is the root mean square of matter fluctuations in spheres of radius 8 h^{-1}Mpc:

$$\sigma_8^2(a) = \int d^3k \, \frac{P_{mm}(k,a)}{2\pi^2} |W(kR)|^2 \tag{28}$$

where

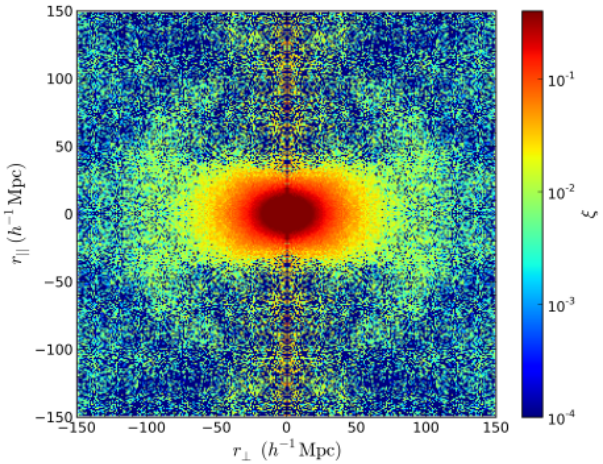
$$W(kR) = \frac{3}{(kR)^3}(\sin(kR) - kR\cos(kR)) \tag{29}$$

Here $R = 8h^{-1}$Mpc and $W(kR)$ is the Fourier transform of the top-hat window function.

- The quantity $f\sigma_8$ is independent of the bias and is a powerful probe of gravity because it is sensitive to the growth of structure and the amplitude of matter fluctuations.

$$\boxed{f\sigma_8(a) = \frac{d\ln\delta(a)}{d\ln a}\sigma_8(a)} \tag{30}$$

$f\sigma_8$ FROM RSD



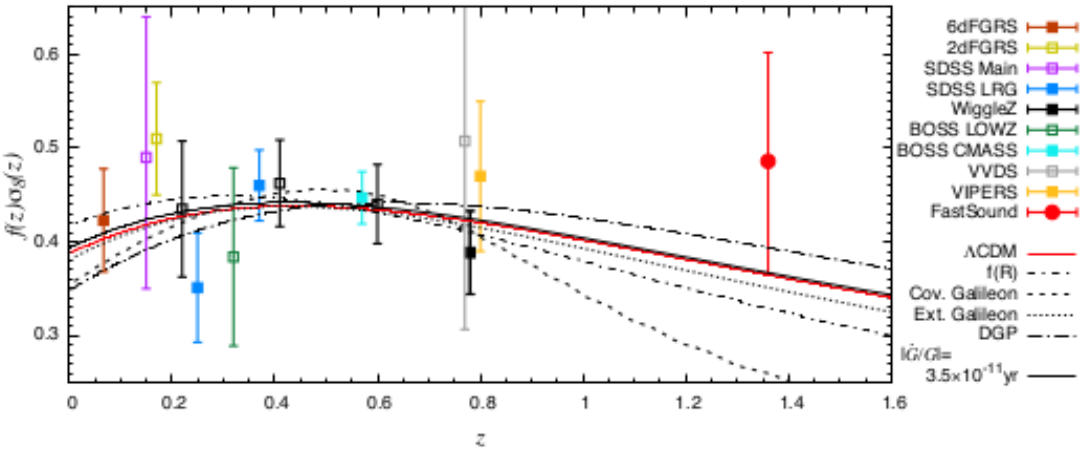


FIGURE: Above: Anisotropic clustering of galaxies in redshift space. Below: Measurements of $(f\sigma_8)$ from different galaxy surveys. (Okumura et al 2016).

$f\sigma_8$ and Galileon Gravity

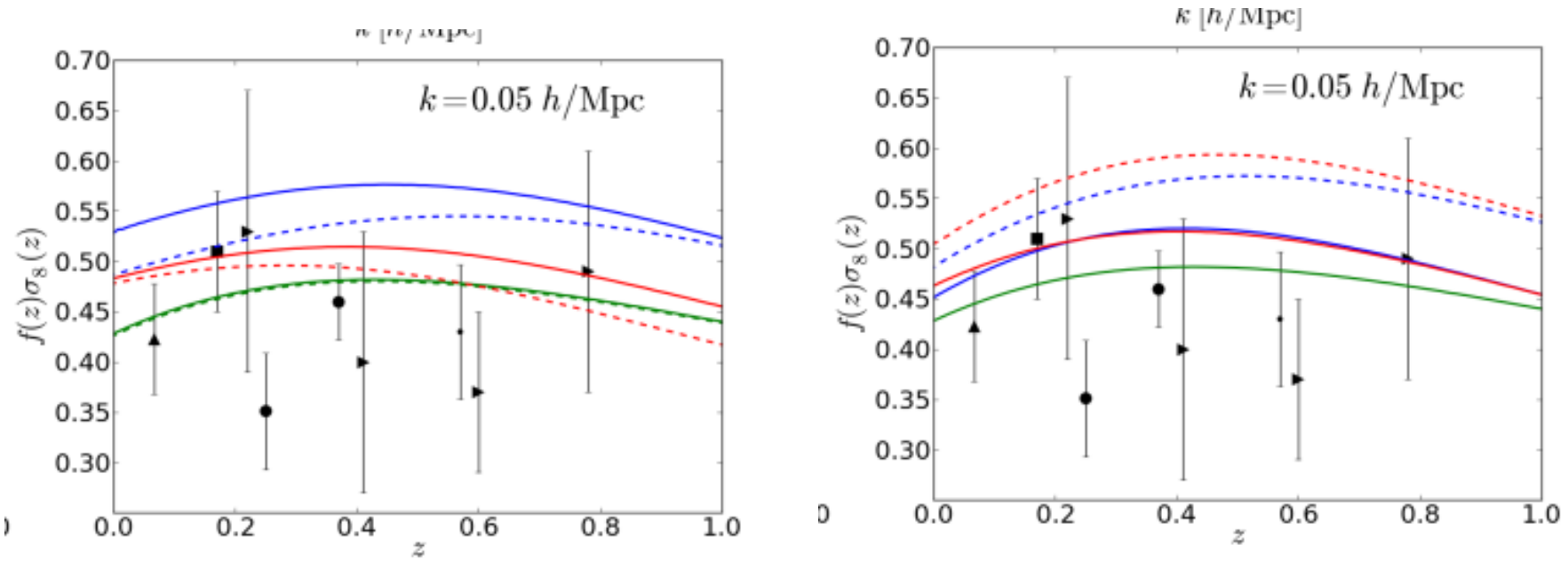


Figure: Best fits models to CMB + CMB lensing + BAO data (solid line). Only CMB + CMB lensing (dashed line) (Barreira et al. 2014)

- Left figure: Green Line: ΛCDM model with massive neutrinos, Blue line: Qubic Galileon, Red lines: Qubic Galileon + Massive neutrinos.
- Right figure: Green Line: ΛCDM model, Blue line: Quintic Galileon, Red line: Cuartic Galileon.

Technical Break

- In ΛCDM, the matter perturbation equation is scale-independent which means in Fourier space:

$$\delta_m(k,a) = f(k)g(a) \qquad \delta'_m(k,a) = f(k)g'(a) \tag{31}$$

- Therefore, the growth rate f is also scale-independent:

$$f(a) = \frac{\partial \ln \delta_m(k,a)}{\partial \ln a} = \frac{\delta'_m(k,a)}{\delta_m(k,a)} a = \frac{g'(a)}{g(a)} a \tag{32}$$

- Also, in ΛCDM, $\sigma_8(a)$ can be expressed as:

$$\sigma_8(a) = \sigma_8 \frac{\delta_m(k,a)}{\delta_m(k,a=1)} a \tag{33}$$

- Finally we get

$$\boxed{f\sigma_8(a) = f(a)\sigma_8(a) = \sigma_8 \frac{\delta'_m(a)}{\delta_m(a=1)} a = \sigma_8 \frac{g'(a)}{g(a=1)} a} \tag{34}$$

- In modified gravity theories, the matter perturbation equation can be scale-dependent which means in Fourier space:

$$\delta_m(k,a) \neq f(k)g(a) \qquad \delta'_m(k,a) \neq f(k)g'(a) \tag{35}$$

- Therefore, the growth rate f is also scale-dependent:

$$f(k,a) = \frac{\partial \ln \delta_m(k,a)}{\partial \ln a} = \frac{\delta'_m(k,a)}{\delta_m(k,a)} \frac{1}{a} \tag{36}$$

- Therefore :

$$f\sigma_8(a) = f(a)\sigma_8(a) = \int k^2 dk\, d\theta\; e^{ika\chi(a)\cos\theta}\; f(k,a) \sin\theta\; \sigma_8(a) \tag{37}$$

However, let us notice that

$$\delta_m(k,a) = \mathcal{R}(\vec{k})T(k,a) \tag{38}$$

where $\mathcal{R}(\vec{k})$ is the primordial curvature perturbation and $T(k,a)$ is the transfer function. However, $\mathcal{R}(\vec{k})$ is not a deterministic quantity, we can only describe it statistically through its power spectrum: $\mathcal{P}_{\mathcal{R}}(k)\delta^3(\vec{k}-\vec{k}') = \langle \mathcal{R}(\vec{k})\mathcal{R}^*(\vec{k}')\rangle$.

Constraints on MG from $f\sigma_8$

- Future RSD (CSST survey) together with Fast Radio Burst measurements of $f\sigma_8$ have been used to forecast constraints on modified gravity asuming a ΛCDM background and using the scale-independent parametrization $\mu(a)$ and $\Sigma(a)$.

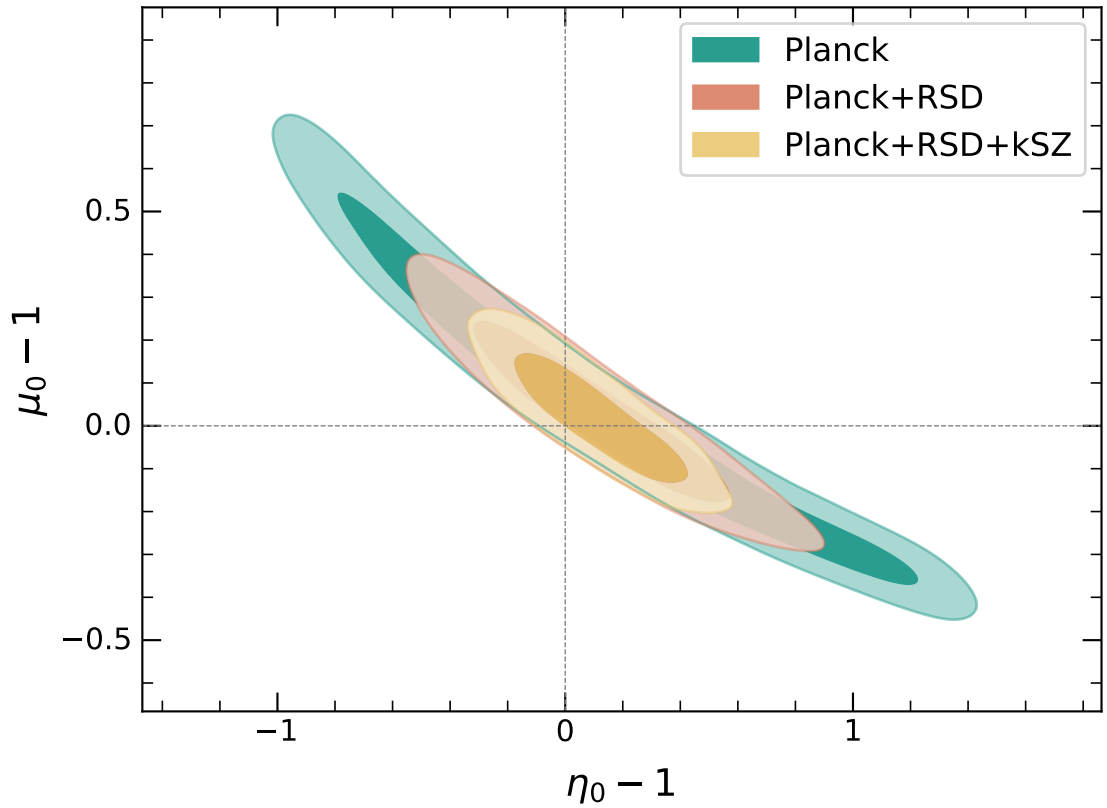


Figure: S. Wang & J. Xia European Physical Journal 85, 414, (2025)

Constraints on MG from $f\sigma_8$

- RSD measurements of $f\sigma_8$ have been used to constrain modified gravity asuming a ΛCDM background and a perturbative $f(T)$ sector with the matter perturbation equation characterized by:

$$\delta_m'' + \left(\frac{3}{a} + \frac{H'}{H}\right)\delta_m' - \frac{3\Omega_{m0}}{2a^5H^2/H_0^2}\frac{G_{\rm eff}}{G}\delta_m = 0 \tag{39}$$

- where $G_{\rm eff}/G$ is given by:

$$\frac{G_{\rm eff}}{G} = \frac{1}{1+F_T} = \frac{1}{1+\frac{\alpha}{2\sqrt{6}H}} \tag{40}$$

Constraints on MG from $f\sigma_8$

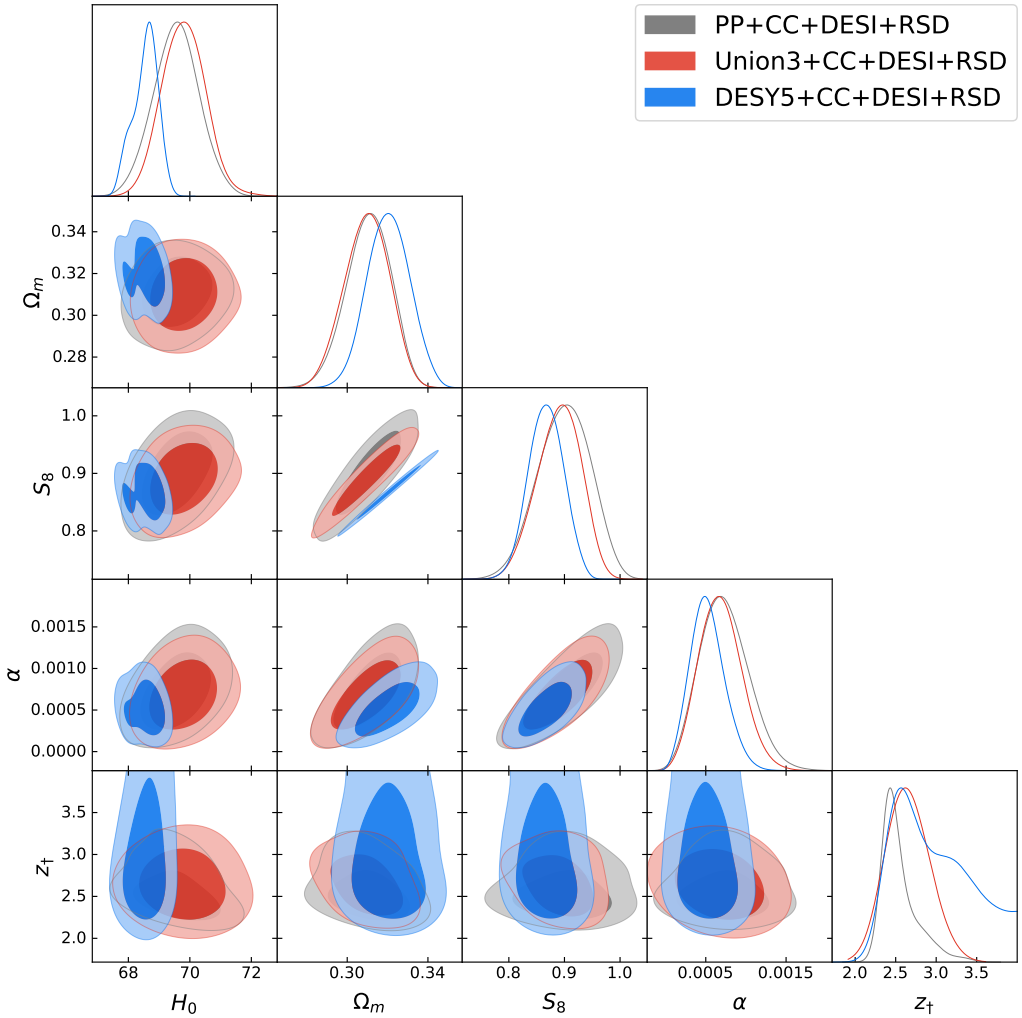


Figure: M.Souza et al. Universe 2025, 11(1), 2

Constraints from DESI DR1 full power shape

- Asuming a ΛCDM background, and a parametrized (MG) model for the perturbations, amd considering only time dependence for μ and Σ:

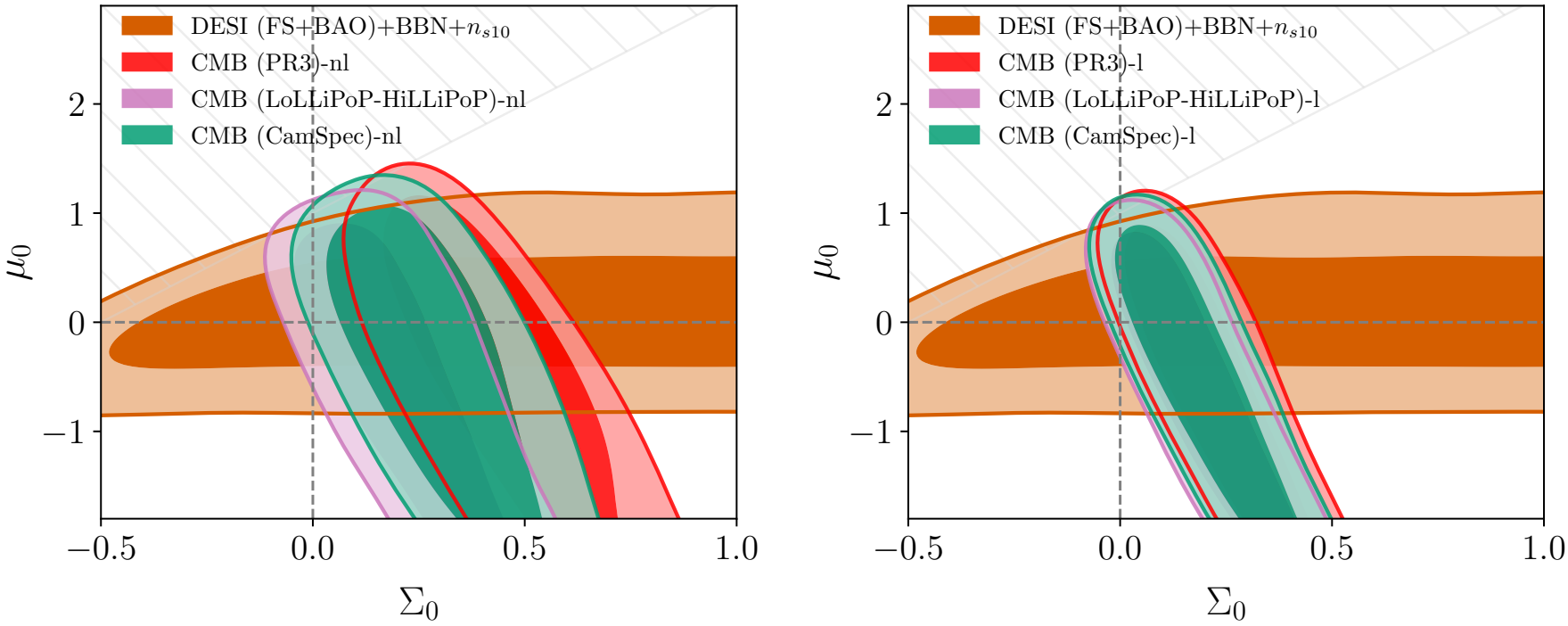
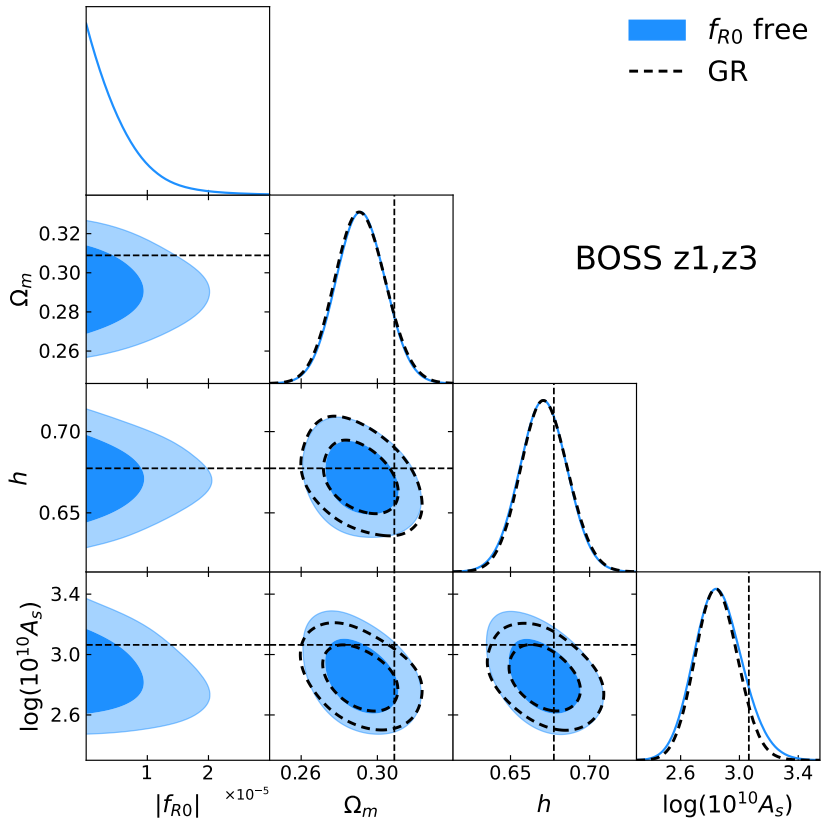


Figure: Constraints on MG models from DESI DR1 M. Ishak et al JCAP09(2025)053: Left: without CMB lensing data, Right: with CMB lensing data

Constraints from FS from BOSS DR12

- Aviles 2024 used the FS of BOSS DR12 to constrain the f_{R0} parameter of Hu-Sawicki $f(R)$ gravity model

$$f_{R0} < 5.89 \times 10^{-6} \quad (68\%\ C.L.) \tag{41}$$



Outline

1 Introduction to Large Scale Structure

2 Galaxy Clustering

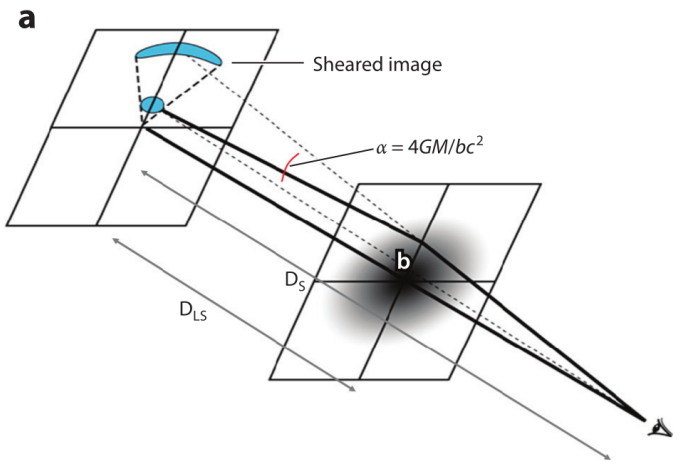
3 Weak Lensing

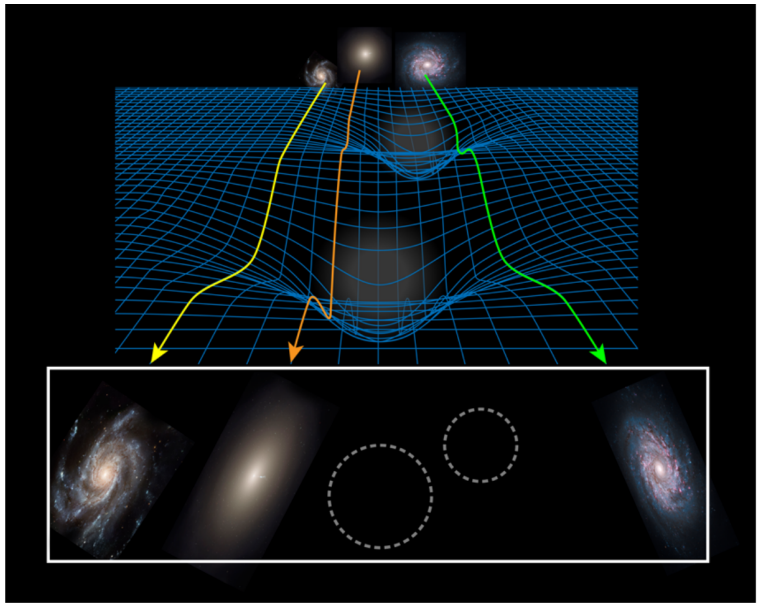
4 Constraints on MG from WL, galaxy surveys and CMB

5 Relevant papers for this lecture

6 Appendix

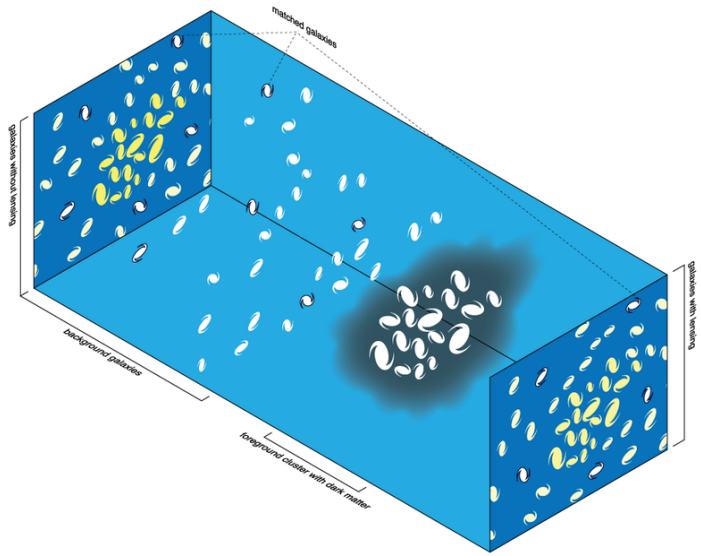
Weak Lensing



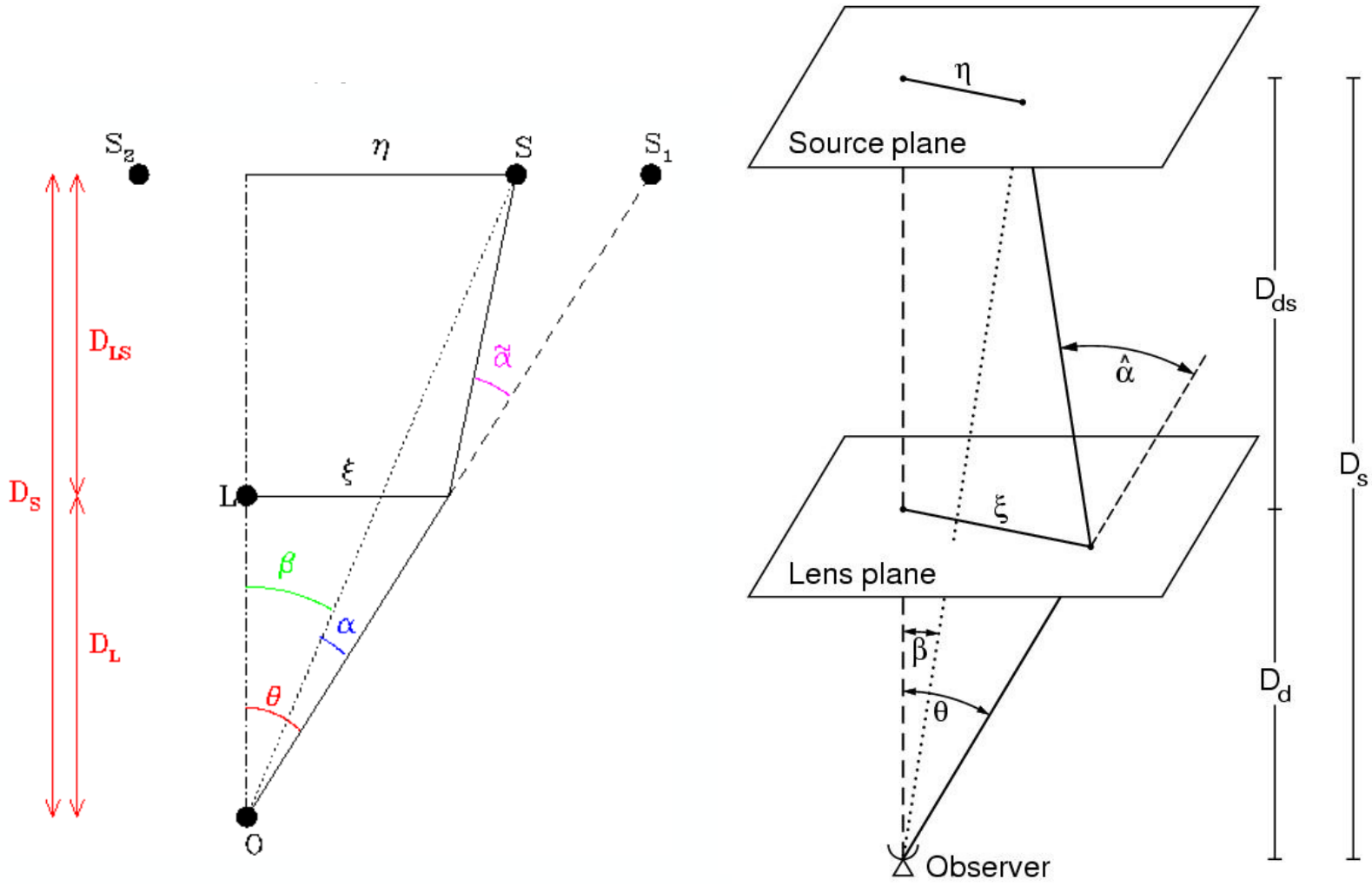


- Gravitational lensing is the deflection of light rays from distant objects by the matter along their path to us.
- In the limit that the deflections cause small modifications of the object properties but not visually striking phenomena such as multiple images or arcs, lensing is referred to as “weak lensing”.
- The correlation function of galaxy shapes is often referred to as cosmic shear.

Cosmic shear surveys



- Cosmic shear surveys (DES, KIDS, HSC, EUCLID, LSST) provide:
  - The angular positions of millions of galaxies (RA,DEC).
  - The redshifts of these galaxies.
  - The shapes of these galaxies. For this high quality images with good angular resolution are required.
- With these measurements the following quantities can be obtained:
  - The shear two-point correlation functions $(\xi_{+/-}(\theta))$.
  - The excess surface density $(\Delta\Sigma(R))$.
  - Details about these quantities will be given in the following slides.



$$\alpha = \nabla_\theta \psi$$

where α is the deflection angle and ψ is the lensing potential.

The lensing potential

- We recall the expression of the lensing potential (ψ):

$$\psi(\theta,\chi) = \frac{2}{c^2}\int_0^{\chi} d\chi' \, \frac{\chi-\chi'}{\chi\chi'}\,\Phi_\gamma(\chi'\theta,\chi') \tag{42}$$

where $\Phi_\gamma = \frac{\Phi_N+\Psi_N}{2}$ is the Weyl potential and $\vec{\theta} = (\theta_1,\theta_2)$

The lensing potential

- We recall the expression of the lensing potential (ψ):

$$\psi(\theta,\chi) = \frac{2}{c^2}\int_0^{\chi} d\chi' \, \frac{\chi-\chi'}{\chi\chi'}\,\Phi_\gamma(\chi'\theta,\chi') \tag{42}$$

  where $\Phi_\gamma = \frac{\Phi_N+\Psi_N}{2}$ is the Weyl potential and $\vec{\theta} = (\theta_1,\theta_2)$

- We recall that the definition of the convergence (κ):

$$\kappa(\vec{\theta}) = \frac{1}{2}\left(\frac{\partial^2\psi}{\partial\theta_1^2} + \frac{\partial^2\psi}{\partial\theta_2^2}\right) = \frac{1}{2}\nabla^2\psi(\vec{\theta}) \tag{43}$$

  This quantity is related to the isotropic magnification of the image

- And also the shear $\gamma = (\gamma_1,\gamma_2)$:

$$\gamma_1(\vec{\theta}) = \frac{1}{2}\left(\frac{\partial^2\psi}{\partial\theta_1^2} - \frac{\partial^2\psi}{\partial\theta_2^2}\right) \quad , \quad \gamma_2(\vec{\theta}) = \frac{\partial^2\psi}{\partial\theta_1\partial\theta_2} \tag{44}$$

  which is related to the anisotropic distortion of the image.

Weak Lensing

- Weak lensing can be described as a linear transformation between unlensed (x_u, y_u) and lensed coordinates(x_l, y_l):

$$\begin{bmatrix} x_u \\ y_u \end{bmatrix} = \begin{bmatrix} 1-\gamma_1-\kappa & -\gamma_2 \\ -\gamma_2 & 1+\gamma_1-\kappa \end{bmatrix} \begin{bmatrix} x_l \\ y_l \end{bmatrix}$$

  Here we remember that the shear $\gamma = (\gamma_1, \gamma_2)$ transformes like a spin-2 quantity and describes the stretching of galaxy images due to lensing. The convergence (κ) describes a change in size and brightness of lensed objects.

- Because we do not know the unlensed distribution of galaxy sizes very precisely, it is common to write this as

$$\begin{bmatrix} x_u \\ y_u \end{bmatrix} = \begin{bmatrix} 1-g_1 & -g_2 \\ -g_2 & 1+g_1 \end{bmatrix} \begin{bmatrix} x_l \\ y_l \end{bmatrix}$$

  where $g_i = \frac{\gamma_i}{1-\kappa}$ is the reduced shear.

- The observed ellipticity is related to the intrinsic ellipticity and the reduced shear as

$$e \approx e_{int} + g \tag{45}$$

  In the weak lensing limit $|g| \ll 1$.

- The estimator for the reduced shear is denoted $\hat{g}$.
- For shear-shear correlations, galaxies are divided into bins based on the photometric redshifts.
- Pairs of galaxies are identified, and their separation on the sky is calculated, including the angle with respect to the sky coordinate axes: separation on the sky θ and polar angle ϕ.
- For each pair, the relevant shear components are tangential $\hat{g}_+$ and cross $\hat{g}_\times$:

$$\begin{aligned} \hat{g}_+ &= -\mathrm{Re}\left[\hat{g}e^{-2i\phi}\right] \\ \hat{g}_\times &= -\mathrm{Im}\left[\hat{g}e^{-2i\phi}\right] \end{aligned}$$

- One of the most popular estimators for the shear two-point correlation functions:

$$\xi_{+/-}(\theta) = < \hat{g}_+\hat{g}_+ > (\theta) \pm < \hat{g}_\times\hat{g}_\times > (\theta) \tag{46}$$

  with $< \hat{g}_+\hat{g}_\times >= 0$ because of the parity symmetry.

Weak Lensing

- The theoretical estimate of the shear two-point correlation functions can be expressed as:

$$\xi^{ij}_{+/-}(\theta) = \frac{1}{2\pi}\int d\ell\, \ell\, \mathcal{J}_{0/4}(\ell\theta) P^{ij}_{\kappa}(\ell) \tag{47}$$

where ij denote tomographic redshift bins, $\mathcal{J}_{0/4}$ are Bessel functions of the first kind, and $P^{ij}_{\kappa}(\ell)$ is the convergence power spectrum for redshift bins ij.

- Using the flat-sky and the Limber approximation, the convergence power spectrum,$P^{ij}_{\kappa}(\ell)$ is written as

$$P^{ij}_{\kappa}(\ell) = \int_0^{\chi_H} d\chi\, q^i(\chi) q^j(\chi) P_{mm}\left(\frac{\ell}{\chi}\right) \tag{48}$$

where χ is the comoving distance, χ_H is the comoving Hubble radius, $P_{mm}(k)$ is the matter power spectrum, and $q^i(\chi)$ is the lensing kernel for the ith redshift bin.

- To test modified gravity models, the power spectra of fields should be derived from the Weyl gravitational potential. Therefore, P_{mm} should be replaced by $k^4 P_{\Phi_\gamma} = k^4 \frac{\psi_N + \phi_N}{2}$ in the above equation. (see the Appendix for exact derivation)

- The lensing kernel $q^i(\chi)$ is given by

$$q^i(\chi) = \frac{3H_0^2\Omega_m}{2c^2}\int_\chi^{\chi_H} d\chi' p^i(\chi')(1+z)\frac{\chi(\chi-\chi')}{\chi'} \tag{49}$$

where $p^i(\chi)$ is the normalized distribution of source galaxies in the ith redshift bin.

Galaxy-Galaxy Clustering

- Galaxy-galaxy clustering is the auto-correlation of the fluctuations of galaxy number density field.
- Using galaxy-galaxy power spectrum $P_{gg}(k)$ and the zero-th order of spherical Bessel function $j_0(x)$, the projected galaxy-galaxy clustering signal is modelled as

$$w_P(R) = 2 \int_0^{\Pi_{max}} d\Pi \, \xi_{gg}(\sqrt{R^2 + \Pi^2}) \tag{50}$$

where R is the transverse comoving separation, and Π is the line-of-sight comoving separation and $\xi_{gg}(r)$ is the three dimensional galaxy clustering

$$\xi_{gg}(r) = \frac{1}{2\pi^2} \int dk \, k^2 P_{gg}(k) j_0(kr) \tag{51}$$

- $w_P(R)$ requires spectroscopic redshifts; integrating over Π removes most of the RSD. Photometric surveys measure $w(\theta)$.

Galaxy-Galaxy Lensing

- In galaxy-galaxy lensing analyses, a sample of foreground galaxies (lenses) is cross-correlated with a sample of background galaxies (sources).
- This is different from cosmic shear, where the background galaxies are lensed by all the matter along the line of sight.
- The observable is the excess surface density $\Delta\Sigma(R)$, which is related to the tangential shear $\gamma_t(R)$ as

$$\Delta\Sigma(R) = \gamma_t(R)\Sigma_c = \bar{\Sigma}(< R) - \Sigma(R) \tag{52}$$

where $\Sigma(R)$ is the surface density at radius R, $\bar{\Sigma}(< R)$ is the mean surface density within radius R, and Σ_c is the critical surface density.

- The theoretical estimate of $\Delta\Sigma(R)$ is given by

$$\Delta\Sigma(R) = \bar{\rho}_m \int_0^\infty \frac{dk}{2\pi} k P_{gm}(k) \mathcal{J}_2(kR) \tag{53}$$

where $P_{gm}(k)$ is the galaxy-matter power spectrum and $\mathcal{J}_2(x)$ is the second-order Bessel function of the first kind.

3×2pt analysis

- The joint analysis of the three two-point functions of the previous slides (cosmic shear, galaxy-galaxy clustering and galaxy-galaxy lensing), measured from the same survey, is called 3×2pt.
- The three probes scale as $b^2\sigma_8^2$, $b\,\sigma_8^2$ and σ_8^2: combining them breaks the bias degeneracy and self-calibrates the shared nuisance parameters (photo-z shifts, shear calibration, intrinsic alignments).
- In MG, lensing responds to the Weyl potential $\Phi_N + \Psi_N$: galaxy-galaxy lensing $\propto (1+\Sigma)$ and cosmic shear $\propto (1+\Sigma)^2$, while galaxy clustering does not depend on Σ. Hence 3×2pt mainly constrains Σ; μ enters only through the growth of P_{mm}.
- Non-Gaussian statistics measurably improve cosmological constraints with real data (Marques et al 2024, Grandón et al 2024, Grandón & Sellentin 2025, Cheng et al 2025).
- Tests of MG combining WL, galaxy-galaxy lensing and galaxy clustering:
  - Simpson et al. MNRAS 429, 2249 (2013): CFHTLenS.
  - Joudaki et al. MNRAS 471, 1259 (2017): KIDS-450.
  - Abbott et al. Phys. Rev. D 99, 123505 (2019): DES-Y1.
  - Abbott et al. Phys. Rev. D 107, 023533 (2023): DES-Y3.

Outline

1 Introduction to Large Scale Structure

2 Galaxy Clustering

3 Weak Lensing

4 Constraints on MG from WL, galaxy surveys and CMB

5 Relevant papers for this lecture

6 Appendix

Latest constraints on MG

- Recalling the following phenomenological parametrizations of MG:

$$\begin{aligned} k^2\Psi_N &= -4\pi G a^2(1+\mu(a,k))\rho\delta \\ k^2(\Phi_N+\Psi_N) &= -8\pi G a^2(1+\Sigma(a,k))\rho\delta \end{aligned} \tag{54}$$

Constraints from CMB, DESI and DES

- Asuming a ΛCDM background, and a parametrized (MG) model for the perturbations, considering only time dependence for μ, Σ and η and using CMB (Planck18), DESI (FS+BAO), WL (DES) and SN (DES):

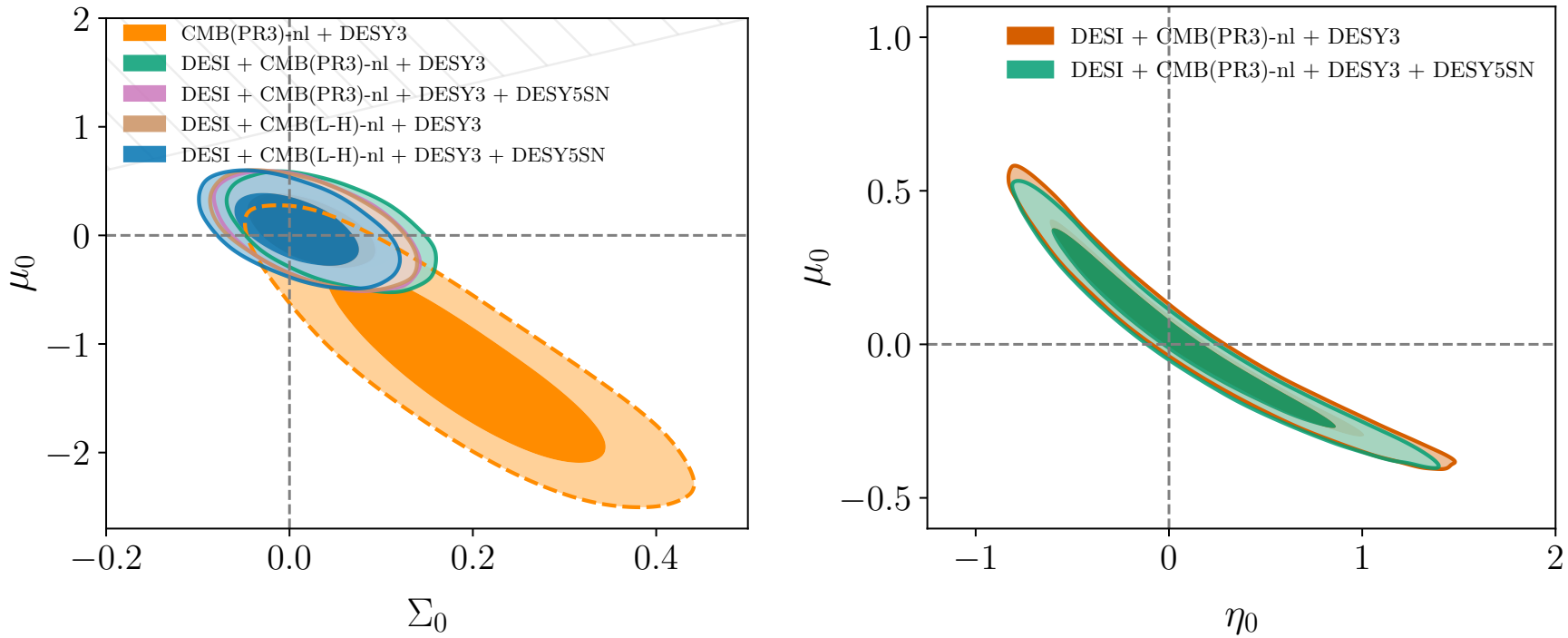


Figure: Constraints on MG models from DESI, CMB and DES (M. Ishak et al JCAP09(2025)053)

Constraints from CMB, DESI and DES

- Asuming a parametric dark energy (w_0, w_a) background, and a parametrized (MG) model for the perturbations, considering only time dependence for μ and Σ :

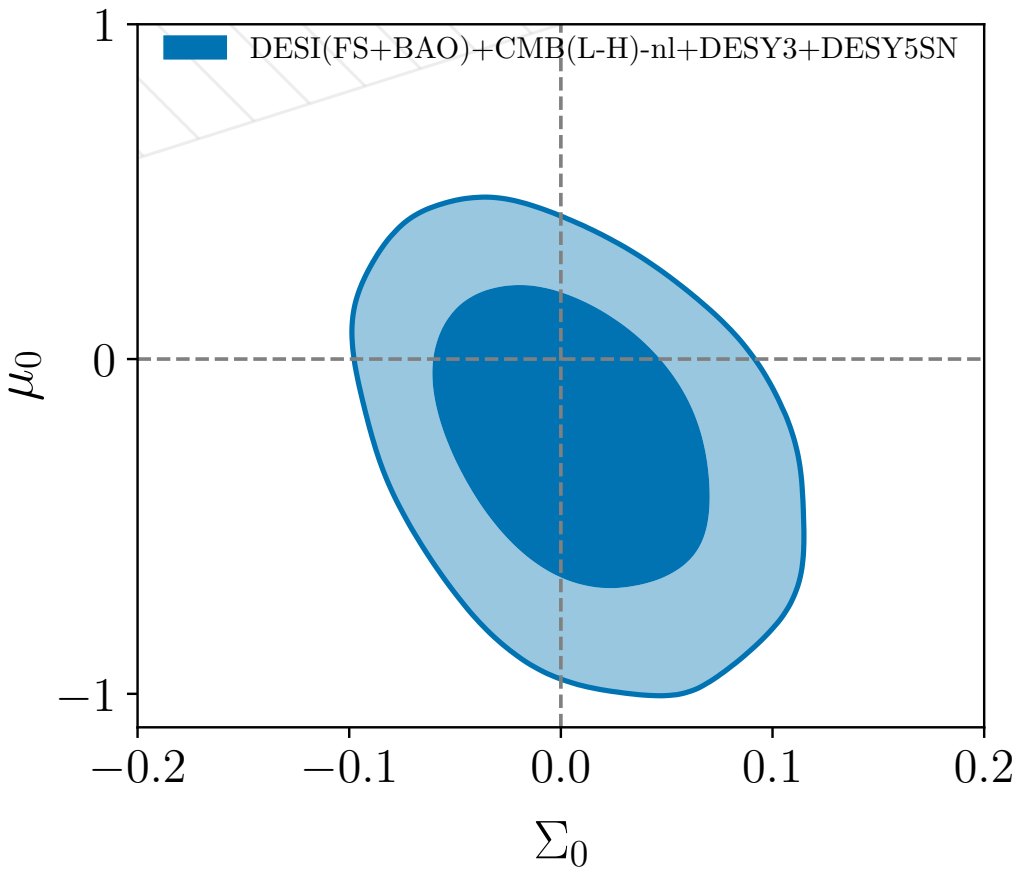


Figure: Constraints on MG models from DESI, CMB and DES (M. Ishak et al JCAP09(2025)053)

- To address the scale dependent case, the following parametrizations are assumed:

$$\mu(a,k) = 1 + \mu_0 \frac{\Omega_{\rm DE}(a)}{\Omega_\Lambda} \left[\frac{1 + c_1 \left(\lambda H(a)/k\right)^2}{1 + \left(\lambda H(a)/k\right)^2} \right] \tag{55}$$

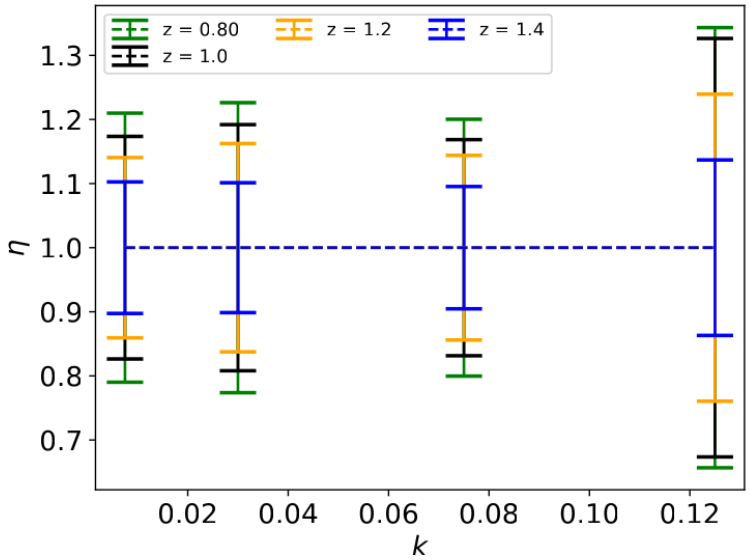
and

$$\Sigma(a,k) = 1 + \Sigma_0 \frac{\Omega_{\rm DE}(a)}{\Omega_\Lambda} \left[\frac{1 + c_2 \left(\lambda H(a)/k\right)^2}{1 + \left(\lambda H(a)/k\right)^2} \right]. \tag{56}$$

Flat LCDM background	μ_0	Σ_0	λ fixed-value	c_1	c_2
DESI+CMB (PR3)-nl +DESY3+DESY5SN	$0.03^{+0.13}_{-0.14}$	0.027 ± 0.043	10	$0.9^{+1.4}_{-1.6}$	—
DESI+CMB (PR3)-nl +DESY3+DESY5SN	$0.12^{+0.14}_{-0.22}$	0.015 ± 0.045	100	$0.7^{+1.1}_{-2.3}$	$0.52^{+0.94}_{-1.4}$

Forecast from WL and galaxy surveys

- Sakr, Zheng & Casas (MNRAS 541, 2978 (2025)) forecast constraints on $\eta = \frac{\Phi_N}{\Psi_N}$ using a combination of galaxy clustering and weak lensing from future surveys like Euclid and DESI.



Summary of this course

- Data sets that allow to test the background solution:
  - Type Ia Supernovae $\longrightarrow$ $(\Omega_m = \Omega_{cdm} + \Omega_b)$
  - Baryon Acoustic Oscillations $\longrightarrow$ $(\Omega_{cdm}, \Omega_b, H_0)$
  - Big Bang Nucleosynthesis $\longrightarrow$ $(\Omega_b h^2)$
  - Cosmic Microwave Background $\longrightarrow$ $(\Omega_{cdm}, \Omega_b, H_0, \tau, n_s, A_s, r)$.
- To put constraints on H_0 using SNIa, one must add an independent measurement of the absolute magnitude of Type Ia Supernovae (for example cepheids from the SH0ES project).
- Data sets that allow to test the growth of structures: Weak Lensing, Galaxy Clustering, Redshift Space Distortions.
- Hints of modified gravity: discrepancies in the growth of structures, cosmic shear measurements, and galaxy clustering observations.
- All data sets but BAO are model independent.

Outline

1. Introduction to Large Scale Structure
2. Galaxy Clustering
3. Weak Lensing
4. Constraints on MG from WL, galaxy surveys and CMB
5. Relevant papers for this lecture
6. Appendix

Relevant papers for this lecture

- Link between theory and observations: S.Arai et al. arXiv: 2212.09094, Hou et al Universe 9, 302 (2023), arXiv: 2306.13726
- Anisotropic galaxy clustering and modified gravity: Song et al. (Phys. Rev. D, 92, 043522 (2015)).
- Weak Lensing: Bartelmann & Schneider, Phys. Rep. 340, 291 (2001), R. Mandelbaum Annu. Rev. Astron. Astrophys. 56, 393 (2018)
- Forecast on Modified Gravity: Sakr, Zheng & Casas (MNRAS 541, 2978 (2025)), arXiv 2501.07477.
- Constraints on Modified Gravity from DESI: M. Ishak et al JCAP09(2025)053, arXiv 2505.07828.
- KiDS-Legacy cosmic shear: A.H. Wright et al. A&A 703, A158 (2025), arXiv:2503.19441.
- KiDS-Legacy consistency and joint constraints with external probes: B. Stölzner et al. A&A 702, A169 (2025), arXiv:2503.19442.
- Linear Redshift Distortions: A.J. S. Hamilton, astro-ph/9708102

Outline

1. Introduction to Large Scale Structure
2. Galaxy Clustering
3. Weak Lensing
4. Constraints on MG from WL, galaxy surveys and CMB
5. Relevant papers for this lecture
6. Appendix

Technical break

- The shear two-point correlation functions can be expressed in terms of the E-mode and B-mode power spectra as:

$$\xi_{+}^{ij}(\theta) = \sum_{\ell \geq 2} \frac{2\ell+1}{4\pi} \frac{2(G_{\ell,2}^{+}(x) \pm G_{\ell,2}^{-}(x))}{\ell^2(\ell+1)^2} \times [C_{\rm EE}^{ij}(\ell) + C_{\rm BB}^{ij}(\ell)], \quad (57)$$

where $x = \cos(\theta)$ and $G_{\ell,2}^{+/-}(x)$ are functions of the associated Legendre polynomials.

- The E-mode and B-mode power spectrum $C_{\rm EE}^{ij}(\ell)$ can be expressed as:

$$C_{\rm EE}^{ij}(\ell) = C_{\kappa\kappa}^{ij}(\ell) + C_{\kappa I_{\rm E}}^{ij}(\ell) + C_{\kappa I_{\rm E}}^{ji}(\ell) + C_{I_{\rm E} I_{\rm E}}^{ij}(\ell) \quad (58)$$

$$C_{\rm BB}^{ij}(\ell) = C_{I_{\rm B} I_{\rm B}}^{ij}(\ell) \quad (59)$$

where $C_{\kappa\kappa}^{ij}(\ell)$ is the convergence power spectrum, $C_{\kappa I_{\rm E}}^{ij}(\ell)$ is the cross-power spectrum between the convergence and the intrinsic alignment E-mode, and $C_{I_{\rm E} I_{\rm E}}^{ij}(\ell)$ and $C_{I_{\rm B} I_{\rm B}}^{ij}(\ell)$ are the intrinsic alignment E-mode and B-mode power spectra, respectively.

- Using the Limber approximation and assuming spatial flatness, the angular power spectra for for cosmic shear and galaxy-galaxy lensing can be written in a general form:

$$C^{ij}_{\mathcal{AB}}(\ell) = \int d\chi \frac{q^i_{\mathcal{A}}(\chi) q^j_{\mathcal{B}}(\chi)}{\chi^2} P_\delta \left(k = \frac{\ell + 0.5}{\chi}, z \right), \tag{60}$$

  where $\{\mathcal{A}, \mathcal{B}\} \in \{\delta_g, \kappa\}$ and κ is the weak lensing convergence. Also, $P_\delta(k, z)$ is the three-dimensional matter power spectrum evaluated at wavenumber k and redshift z.

- To test modified gravity models, the power spectra of fields should be derived from the Weyl gravitational potential. Therefore, $P_\delta(k, z)$ should be replaced by $k^4 P_{\Phi_\gamma}(k, z)$ in the above equation.

Measuring β: angle-averaged $P(k)$

- The Kaiser formula is usually written in terms of the linear redshift distortion parameter β:

$$P^s(\mathbf{k}) = (1 + \beta\mu_k^2)^2 P(k)\,, \qquad \beta = \frac{f}{b} \tag{61}$$

where P^s is the redshift-space spectrum, P its real-space (unredshifted) counterpart, and μ_k is the cosine of the angle between $\mathbf{k}$ and the line of sight.

- The simplest way to measure β is to average $P^s(\mathbf{k})$ over all directions, $P^s(k) \equiv \int P^s(\mathbf{k})\, do_{\mathbf{k}}/(4\pi)$. Since $\langle\mu_k^2\rangle = 1/3$ and $\langle\mu_k^4\rangle = 1/5$, the angular average of $(1 + \beta\mu_k^2)^2$ gives a constant amplification:

$$\frac{P^s(k)}{P(k)} = 1 + \frac{2}{3}\beta + \frac{1}{5}\beta^2 \tag{62}$$

The amplification is independent of k: the redshift-space spectrum has the same shape as the real-space one, only a larger amplitude.

- As β varies between 0 and 1, the amplification factor varies between 1 and $28/15$, almost a factor of 2. (Hamilton 1997)

Measuring β: smoothed power spectra

- The previous result holds for any wavenumber k in the linear regime. Therefore it remains valid if both spectra are first smoothed over a window $W(k)$ that selects only linear wavenumbers:

$$\tilde{P}(k) \equiv \int_0^\infty W(k) P(k) \frac{4\pi k^2 dk}{(2\pi)^3} \tag{63}$$

and similarly for $\tilde{P}^s(k)$.

- The ratio of the smoothed redshift-space to real-space spectra obeys the same relation:

$$\frac{\tilde{P}^s}{\tilde{P}} = 1 + \frac{2}{3}\beta + \frac{1}{5}\beta^2 \tag{64}$$

- This is useful in practice: smoothing reduces the noise of the measurement, and lets one filter out the non-linear scales where the Kaiser formula breaks down, without changing the predicted amplification.

Measuring β: the correlation function

- Choosing the smoothing window to be the zeroth spherical Bessel function, $W(k) = \int e^{-i\mathbf{k}\cdot\mathbf{r}} do_{\mathbf{k}}/(4\pi) = j_0(kr)$, the smoothed spectrum becomes the correlation function.
- Hence the ratio of the angle-averaged redshift-space correlation function $\xi^s(r) \equiv \int \xi^s(\mathbf{r})\, do_{\mathbf{r}}/(4\pi)$ (the monopole $\xi^s_0(r)$) to its real-space counterpart $\xi(r)$ is, at linear separations r:

$$\frac{\xi^s(r)}{\xi(r)} = 1 + \frac{2}{3}\beta + \frac{1}{5}\beta^2 \tag{65}$$

  i.e. exactly the same amplification factor, now in configuration space.
- Caveat: all these estimators require the real-space quantity $\xi(r)$ or $P(k)$, which has to be obtained by deprojecting the angular correlation function of the survey. This deprojection is quite noisy unless the survey is large, which limits the precision of β measured in this way.
- This motivates the alternative method of §5.2: the ratio of the quadrupole to monopole moments of P^s, which needs no real-space reference.

Multipoles of the redshift-space $P(k)$

- In the plane-parallel approximation, $P^s(\mathbf{k})$ can be expanded in even Legendre multipoles $P^s_\ell(k)$:

$$P^s(\mathbf{k}) = \sum_{\ell \text{ even}} \mathcal{P}_\ell(\mu_k) P^s_\ell(k)\,, \qquad P^s_\ell(k) \equiv (2\ell+1) \int \mathcal{P}_\ell(\mu_k) P^s(\mathbf{k})\, do_{\mathbf{k}}/4\pi \tag{66}$$

  where $\mathcal{P}_\ell$ are the Legendre polynomials (not to be confused with the spectra P^s_ℓ). The odd multipoles vanish by pair-exchange symmetry, and the $m \neq 0$ azimuthal ones by symmetry about the line of sight.

- In the linear regime, Kaiser's formula contains only powers $\mu_k^0, \mu_k^2, \mu_k^4$, so the sum truncates at the hexadecapole: only monopole ($\ell = 0$), quadrupole ($\ell = 2$) and hexadecapole ($\ell = 4$) survive:

$$P^s(\mathbf{k}) = \mathcal{P}_0(\mu_k) P^s_0(k) + \mathcal{P}_2(\mu_k) P^s_2(k) + \mathcal{P}_4(\mu_k) P^s_4(k) \tag{67}$$

The linear multipoles

- Expanding $(1+\beta\mu_k^2)^2$ in Legendre polynomials relates each multipole to the same real-space spectrum $P(k)$:

$$\begin{aligned} P_0^s(k) &= \left(1+\frac{2}{3}\beta+\frac{1}{5}\beta^2\right)P(k) \\ P_2^s(k) &= \left(\frac{4}{3}\beta+\frac{4}{7}\beta^2\right)P(k) \\ P_4^s(k) &= \frac{8}{35}\beta^2 P(k) \end{aligned} \tag{68}$$

- The monopole reproduces the constant amplification of eq. (13), while the higher multipoles are pure RSD: they vanish if $\beta = 0$. All of them share the same shape $P(k)$, and differ only in amplitude.

The quadrupole-to-monopole ratio

- Since $P(k)$ is common to all the multipoles, it cancels in the ratio, which therefore depends only on β:

$$\frac{P_2^s(k)}{P_0^s(k)} = \frac{\frac{4}{3}\beta + \frac{4}{7}\beta^2}{1 + \frac{2}{3}\beta + \frac{1}{5}\beta^2} \tag{69}$$

  This provides a means of measuring β with no need of the real-space $P(k)$, avoiding the noisy deprojection required by method 1.

- The hexadecapole is predicted to be small, $\lesssim 0.1$ of the monopole and quadrupole for $\beta \leq 1$, and it is also noisier, especially at the largest scales.

- Hence, in practice, the quadrupole-to-monopole ratio has been the statistic of choice for many authors. (Hamilton 1997)